Engineering an Insulating Ferroelectric Superlattice with a Tunable Band Gap from Metallic Components

Saurabh Ghosh, Albina Y. Borisevich, and Sokrates T. Pantelides

Phys. Rev. Lett. **119**, 177603 — Published 25 October 2017

DOI: 10.1103/PhysRevLett.119.177603

Engineering an insulating ferroelectric superlattice with tunable band gap from metallic components

Saurabh Ghosh[1,2],* Albina Y. Borisevich[2], and Sokrates T. Pantelides[1,2]
[1] *Department of Physics and Astronomy, Vanderbilt University, Nashville, Tennessee 37235, USA and*
[2] *Materials Science and Technology Division, Oak Ridge National Laboratory, Oak Ridge, Tennessee 37831, USA*
(Dated: August 29, 2017)

The recent discovery of 'polar metals' with ferroelectric-like displacements offers the promise of designing ferroelectrics with tunable energy gaps by inducing controlled metal-insulator transitions. Here we employ first-principles calculations to design a metallic polar superlattice from non-polar metal components and show that controlled intermixing can lead to a true insulating ferroelectric with tunable band gap. We consider a 2/2 superlattice made of two centrosymmetric metallic oxides, $La_{0.75}Sr_{0.25}MnO_3$ and $LaNiO_3$, and show that ferroelectric-like displacements are induced. The ferroelectric-like distortion is found to be strongly dependent on the carrier concentration (Sr content). Further, we show that a metal-to-insulator (MI) transition is feasible in this system via disproportionation of the Ni sites. Such a disproportionation and hence a MI transition can be driven by intermixing of transition metal ions between Mn and Ni layers. As a result, the energy gap of the resulting ferroelectric can be tuned by varying the degree of intermixing in the experimental fabrication method.

Ferroelectrics are insulating materials with spontaneous microscopic polarization, which can be reversed by the application of an electric field [1, 2]. However, in 1965, Anderson and Blount first suggested that polar displacements, which drive a material from a high-symmetry paraelectric phase to a low-symmetry ferroelectric phase, could exist in a metal [3]. Recently, the observation of a ferroelectric-like structural transition in the metallic oxide $LiOsO_3$ [4] generated an interest in polar metals [5–11]. Fundamentally, there is no incompatibility between metallicity and polar or ferroelectric-like displacements [5]. However, successful coupling between an external electric field and polarization requires that the system is an insulator because a nonzero electric field cannot be sustained in a metal. The question then arises if it is possible to design a material that undergoes a transition from a ferroelectric-like metallic (FEL/M) phase to a true ferroelectric insulating (FE/I) phase. The mechanism that underlies such a transition would reveal options for the design of ferroelectrics with tunable energy gaps.

To achieve a transition from a FEL/M phase to a FE/I phase, two conditions need to be satisfied: First, the polar displacements need to be present in both phases and second, the system has to acquire a metal-to-insulator transition. In this context, interfaces between metallic oxides can be compelling, as transition-metal oxide (TMO) heretostructures in the perovskite architecture offer many functional properties including metal-insulator transitions, ferroelectricity, magnetoresistance, etc. [12–22]. In the context of ferroelectricity (FE), the appearance of an electrical polarization is usually driven by a second-order Jahn-Teller (SOJT) mechanism [2]. However, recent studies have shown that, with proper choice of materials and by taking advantage of heterostructures, alternative mechanisms are also possible [13–15, 22]. TMO heretostructures are equally promising for metal-insulator transition, as conductivity has been shown strongly driven by structural and electronic asymmetries at the interface [17, 21]. In particular, charge transfer between two dissimilar interfaces was reported to induce either ferroelectricity or metal-insulator transition in different systems [15, 17]. Thus, TMO heterostructures built from metallic components are certainly a promising starting point where the possibility of a FEL/M-to-FE/I transition can be explored.

In this paper, we use first-principles density-functional-theory (DFT) calculations to consider superlattices (SLs) constructed from metallic components and formulate a mechanism to functionalize a polar metal into an insulating ferroelectric with tunable energy gap. We investigated short-period SLs of the form $(La_{0.75}Sr_{0.25}MnO_3)_m/(LaNiO_3)_n$, where, m/n = 1/1, 2/2, 3/1. The 2/2 SL was found to be a polar metal (i.e., FEL/M phase) that can undergo a metal-insulator transition. The trigger for such a metal-insulator transition is a small disproportionation of the oxidation state on the Ni sites. In the case of 2/2 SL, disproportionation can be brought about by Mn/Ni intermixing, a phenomenon that is known to occur in similar systems. Finally, we have found that the polar mode in the non-intermixed 2/2 superlattice strongly depends on the concentration of delocalized holes in the system, which can lead to a new family of tunable polar metals.

First-principles calculations were carried out using density functional theory [23] with projector augmented wave (PAW) potentials [24]. We used the rotationally invariant LSDA+U approach introduced by Liechtenstein et. al. [25, 26], as implemented in the Vienna ab initio simulation package (VASP) [27]. We have included the on-site $d-d$ static Coulomb interaction parameter U using values $U_{Mn} \leq 2$ and $U_{Ni} \leq 6$, as determined by a procedure described in Supplemental Information,

Figs. S1b and S1c. More specifically, calculations were done using U_{Mn}=0.5 eV, and Ni, U_{Ni}=6.0 eV with an exchange interaction parameter J=1.0 eV, but key results were tested using values U_{Mn} =1.5 eV and U_{Mn} =2 eV and were found to remain unchanged (see below). The exchange-correlation part is approximated by the PBEsol functional [28]. The total energy and Hellman-Feynman force were converged to 1.0 μeV and 1.0 meV/Å, respectively. Various supercells have been constructed for this study. In case of non-intermixed structures, a $\sqrt{2}a_p \times \sqrt{2}a_p \times 4a_c$ supercell has been used. We have fixed the in-plane lattice to cubic $SrTiO_3$ (3.905 Å) and c lattice parameter was optimized. In the case of intermixed structures, a series of supercells has been constructed to represent different scenarios of intermixing.

Our aim is to design a ferroelectric superlattice from metallic oxide interfaces. We have chosen $(La_{0.75}Sr_{0.25}MnO_3)_m/(LaNiO_3)_n$SLs (LSMO/LNO) as both $La_{0.75}Sr_{0.25}MnO_3$ and $LaNiO_3$ are metallic oxides while their electronic structure, i.e., the presence of delocalized and/or ligand holes induced by TM_{3d}-O_{2p} hybridization may lead to an insulating or near insulating state [29–33]. Furthermore, it was recently reported that a metallic interface can drive a hidden ferroelectric-like distortion [34]. In bulk $La_{1-x}Sr_xMnO_3$ (where, x is concentration of holes), A site is populated randomly by La^{3+} and Sr^{2+} cations which lead to B-cations to have a mixed-valence of $Mn^{3+}(d^4)/Mn^{4+}(d^3)$, with $x = 0.25$, the system is reported to be antiferromagnetic metal [29, 30]. On the other hand, $RNiO_3$ family undergoes metal-insulator (MT) transition driven by NiO_6 octahedral distortions associated with complex charge disproportionations. In case of $LaNiO_3$, this transition occurs at 40 K [31–33]. In the present study we have considered the metallic Pnma structure of $LaNiO_3$, in which a charge disproportionation mode is absent. Thus, both of our building blocks, LSMO and LNO, are metallic.

In Figure1(a), and (b), we show the high-symmetry $P4/mmm$ and lowest-energy Pm structures of a 2/2 SL, respectively. To relate the high-symmetry $P4/mmm$ to the low-symmetry Pm phase through a group-subgroup relation, we have performed phonon calculations on the $P4/mmm$ structure in the ferromagnetic (FM) magnetic configuration (supplementary information-II). The dominant structural distortions in $P4/mmm$ were found to be driven by octahedral rotations. However, with the set of parameters U_{Mn}=0.5 eV, U_{Ni}=6.0 eV and J=1.0 eV, the lowest-energy magnetic state is found to be antiferromagnetic (AF) for both structures. The AF configuration is such that individually the Mn and Ni sublattices have A-type AF alignment, while at the interface the Mn-O-Ni coupling is FM, resulting in alternating magnetic moments for neighboring interfaces and zero net magnetization. We will denote this configuration as AFA (supporting information III). This particular AFA-type magnetic ordering is also found to be the lowest-energy magnetic configuration for the $(LaMnO_3)_2/(LaNiO_3)_2$ superlattice [35–38].

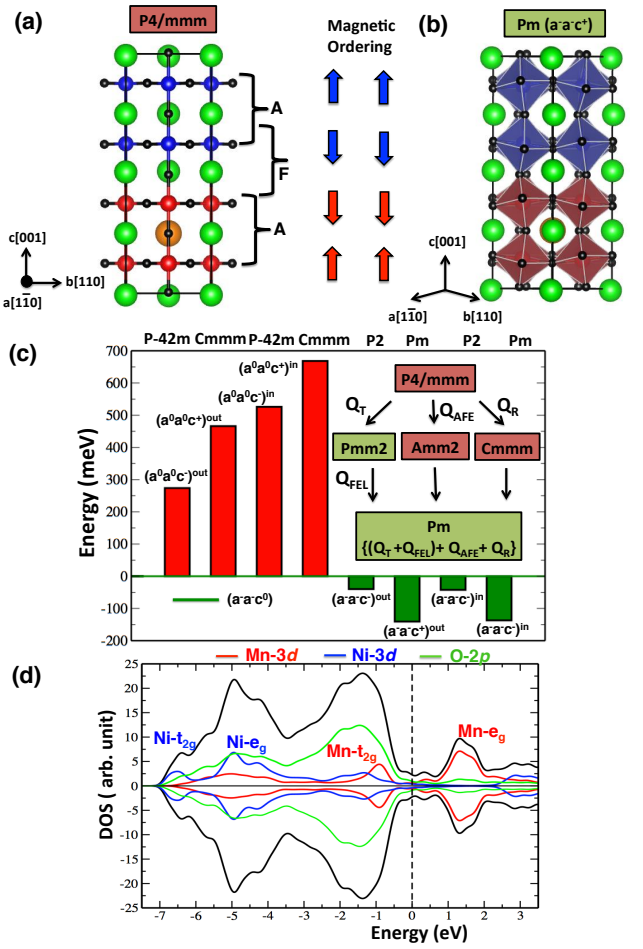

FIG. 1. Structural and electronic properties of 2/2 SL. (a) & (b) High symmetry $P4/mmm$ and lowest energy Pm structures, respectively. Green, orange, read, blue and black balls represents La, Sr, Mn, Ni and O atoms, respectively. The magnetic configuration AFA implies that Mn and Ni sublattices are aligned AFA-type while at the interface the Mn-O-Ni coupling is ferromagnetic. (c) Relative energetics of dominant distortions with respect to $a^-a^-c^0$ (Q_T) distortion. Here, 'in' and 'out' represent 'in phase' and 'out of phase' sense of rotation of BO_6 octahedra at the interface (Supplementary Information-II). The polar space groups are shown in green. (d) Density of states (DOS) calculated for U_{Mn} =0.5 eV, U_{Ni} =6.0 eV and J= 1.0 eV.

When considered individually, the distortion mode corresponding to the lowest energy has $Pmm2$ space group, which has $a^-a^-c^0$ rotation. Other BO_6 octahedral distortions are found to be much higher in energy, as shown in Figure1(c). The symmetry of the lowest-energy Pm phase is established by two symmetry-lowering structural distortions of the tetragonal $P4/mmm$ perovskite structure:an out of phase tilt of the BO_6 octahedra (Q_T, Glazer notation [39] $a^-a^-c^0$) about the cubic [110] axis

and an in-phase rotation of the BO_6 octahedra (Q_R, Glazer notation $a^-a^-c^0$) about the cubic [001] axis. Together these distortions stabilize the $a^-a^-c^+$ rotation pattern via. a trilinear coupling of the from $\mathcal{F} \sim Q_T\ Q_R\ Q_{AFE}$, where Q_{AFE} is the anti-ferroelectric A-cation displacement. Here, to note that in case of bulk $La_{0.75}Sr_{0.25}MnO_3$ the rotation pattern is $a^0a^0c^-$. However, in case of 2/2 SL the rotation pattern is $a^-a^-c^+$ as there is an additional energy gain due to trilinear coupling.

Considering the electronic structure, Pm-AFA phase is found to be metallic as shown by the density of states (DOS) plot in Figure1(d). In case of a pure Mn (4+)/Ni (2+) system with ($3d^3$: $t_{2g}^3e_g^0/3d^8$: $t_{2g}^6e_g^2$) electronic configuration, the system is expected to be an insulator. However, from previous theoretical studies on $(LaMnO_3)_2$ / $(LaNiO_3)_2$ SL, it was predicted that the system remains metallic and additional structural distortions are required to remove this portion of DOS from fermi level (E_f) [40]. In case of 2/2 SL due to presence of a delocalized hole (a La^{3+} ion has been replaced by a Sr^{2+} in the unit cell) both Mn and Ni becomes slightly mixed valance and TM_{3d}-O_{2p} hybridization give rise to finite DOS at the E_f. All other intermediate metastable phases also show similar electronic structure and thus remain metallic.

Here we note that the lowest-energy phase Pm ($a^-a^-c^+$) and the intermediate phase $Pmm2$ ($a^-a^-c^0$) are in non-centrosymmetric space groups and thus can be polar. Further analysis of phonon modes reveals a 'ferroelectric-like' (FEL) mode as shown in Figure2(a). Due to $a^-a^-c^0$ (Q_T) mode, both La^{3+} and apical O^{2-} ions are displaced from their respective centrosymmetric positions. In the case of a 2/2 SL, the magnitude of displacements of La^{3+} and apical O^{2-} in the $LaNiO_3$ block is significantly larger when compared to other layers due to coupling between Q_T and FEL. Due to the absence of coupling with the FEL mode, an intermediate $Cmmm$ phase that represents a $a^0a^0c^+$ (Q_R) rotation remains centrosymmetric. When we 'freeze in' the amplitude of the FEL mode and compute the corresponding total energy as a function of the mode amplitude, a double well potential is obtained as shown in Figure2(b). The FEL mode couples to Q_T and, together, these two distortions (Q_T + FEL) establish a polar space group. Reversing the sense of Q_T can also reverse the direction of the FEL mode.

A Similar type of asymmetric distortion has been shown to lead ferroelecricity with a net measurable in plane polarization for $(YTiO_3)_2/(YFeO_3)_2$ and $(LaTiO_3)_2/(LaVO_4)_2$ magnetic superlattices. Charge transfer across the interface is reported to be the origin of such ferroelectric mode [11, 15]. Moreover, the FEL mode in a 2/2 SL demonstrates strong carrier concentration dependence, which is also a key characteristic of a polar metal [5]. However, in the case of a 2/2 SL,

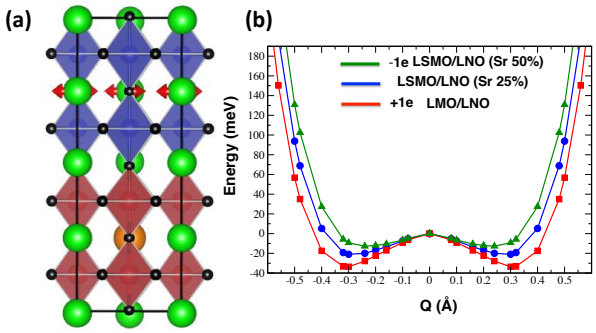

FIG. 2. (a) Schematic depiction of the ferroelectric-like (FEL) mode and (b) Carrier concentration (Sr content) dependency of the FEL mode distortion. Green, orange, red, blue and black spheres represent La, Sr, Mn, Ni and O atoms, respectively.

the lowest-energy Pm phase remains metallic and the polarization cannot be measured using the Berry-phase method. We, therefore, refer to this mode as 'ferroelectric like'.

As both the individual building blocks are metallic as illustrated in Figure 3(a) and the pristine 2/2 SL is also metallic as shown by the DOS is Figure 1(d), the important question now is how to open a gap so that the polarization becomes measurable. We note that the double perovskite La_2MnNiO_6 is insulating both in the orthorhombic and the monoclinic structure, with the Mn and Ni ions ordered in a rocksalt pattern [41]. Hence, two questions arise: (a) Can Mn/Ni intermixing open an energy gap in the 2/2 SL? And, if an energy gap opens up, (b) will the ferroelectric mode persist and can the ferroelectric polarization be measured in an intermixed structure? To explore the effect of intermixing we have considered various types of ordered intermixing (computational constraints do not allow us to consider disordered intermixing, but the results suggest that disorder would not change the main conclusions; supplementary information-IV). The results are summarized in Table 1. For a 25% intermixing concentration, the lowest-energy

TABLE I. Finite band gap (B.G) and polarization (when ferroelectric) of $(La_{1-x}Sr_xMnO_3)_m/(LaNiO_3)_n$ superlattices (LSMO/LNO SLs). Metal-insulator transition has dual origin i.e, intermixing and charge disproportionation (CDP).

$(LSMO)_m$ / Sr doping (x%)	$(LNO)_n$ SL Period (m/n)	Intermixing (%)	CDP	Finite B.G (eV)	Polarization ($\mu C/cm^2$)
50	1/1	No	Yes	0.25	No
25	2/2	No	No	No	No
		12.5	Yes	No	No
		18.75	Yes	0.09	4.21
		25	Yes	0.51	9.31
16.67	3/1	No	No	No	No

configuration is shown in Figure 3(b), which we define as 'column intermixing'. The intermixed structure is found to be much lower in energy (∼0.35 eV) compared to the pristine interface [37]. Though this result means that intermixing is an exothermic process, employing kinetic constraints during growth can control the amount of intermixing. Gibert et al. in Ref. [19, 37] have demonstrated that, by controlling the growth conditions and temperature, it is possible to control the degree of intermixing in experiments.

As shown in Figure 3(c), after structural relaxation, Ni sites are no longer equivalent, forming Ni_1 and Ni_2. At the Ni_1 sites, the NiO_6 octahedron is slightly contracted, while at the Ni_2 sites, the octahedron is slightly elongated in the crystallographic *ab*-plane. The presence of two different types of Ni sites has also been confirmed by calculating local magnetic-moments. For an ideal interface without intermixing the magnetic moment on each Mn and Ni is found to be 2.64 μ_B and 1.54 μ_B, respectively. In the case of 25% intermixing, Ni sites have two distinct magnetic moments of 1.70 μ_B and 1.31 μ_B for Ni_2 and Ni_1, respectively.

The above results indicate that the cause of the symmetry breaking is disproportionation of the Ni oxidation states. The difference between the two resultant oxidation states is not large; the respective oxidation states can be thought of as $+2 \pm \delta$. However, this change is enough to generate $p-d$ repulsion and remove finite DOS from E_F, opening a energy gap of magnitude 0.51 eV as shown in Figure 3(d). In order to check that this result is not sensitive to the value of U_{Mn}, we optimized the 25%-intermixed and non-intermixed structures using U_{Mn} = 1.5 eV, U_{Ni} = 6.0 eV and J=1.0 eV. The conclusions remain unchanged i.e. the non-intermixed structure is a polar metal and the 25%-intermixed structure is an insulating ferroelectric (with band gap 0.4 eV). Here, the metal-insulator transition may be viewed as being driven by an internal volume collapse where one NiO_6 octahedron shrinks around its central Ni, while the other octahedron expands accordingly. Similar behavior has been reported for $LaNiO_3$ in Ref. [31]. However, in this present case the electronic driven charge disproportionation could be related to the presence of a of a differently sized cation (Mn) in the Ni layer

We have found that, in the case of a $La_{0.75}Sr_{0.25}MnO_3/LaNiO_3$ 2/2 SL, a critical level of intermixing (∼18.75%) is required to open a gap (see Table I). Conversely, in a $La_{0.5}Sr_{0.5}MnO_3$/ $LaNiO_3$ 1/1 SL , Ni sites undergo charge disproportionation without any intermixing, opening a gap of 0.25 eV. Therefore, in $(La_{1-x}Sr_xMnO_3)/(LaNiO_3)$ superlattices, the metal-insulator transition is governed by a complex interplay of disproportionation, carrier concentration and intermixing. In the case of a 2/2 SL, due to intermixing-driven disproportionation, the metallic *Pm* phase converts into an insulating *P*1 phase. Once we

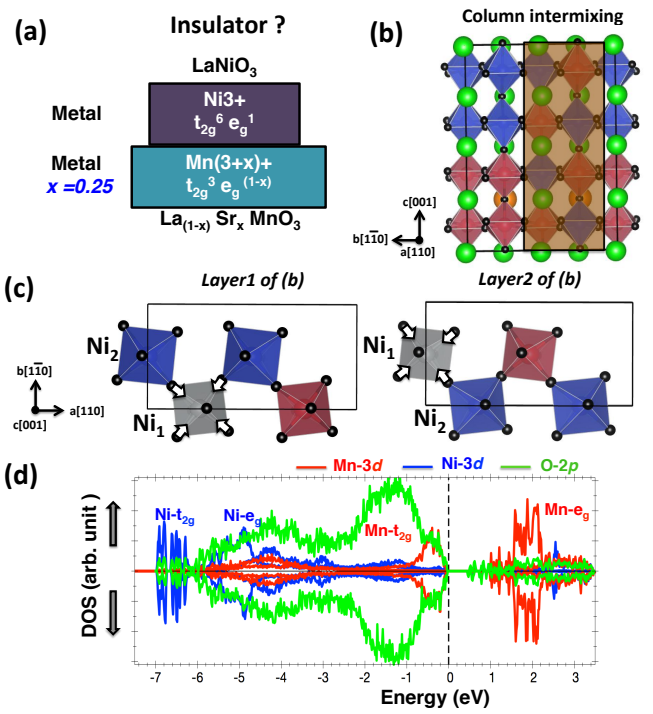

FIG. 3. (a) Engineering a metal-insulator transition in a superlattice of two metallic oxides. (a) Schematic representation of the problem. (b) Column intermixing configuration, (c) Two nonequivalent NiO_6 octahedra arising from charge disproportionation. At the Ni_1 sites, the NiO_6 octahedron is slightly contracted, (as indicated by white arrows) while at the Ni_2 sites, the octahedron is slightly elongated in the crystallographic *ab*-plane. White arrows highlight the compressed NiO_6 octahedra. (c) DOS for intermixed structure computed for U_{Mn} =0.5 eV, U_{Ni} =6.0 eV and J= 1.0 eV. Here, Green, orange, red, blue and black spheres represent La, Sr, Mn, Ni and O atoms, respectively.

are able to open the energy gap, we are able to measure the total (atomic + electronic) ferroelectric polarization using the Berry-phase method. We have found that, for 25% and 18.75% intermixing, the calculated polarizations are $9.31\mu C/cm^2$ and $4.21\mu C/cm^2$, respectively, with the polarization vector in the crystallographic *ab* plane.

One of the key characteristics of ferroelectricity is switching of the polarization. In the case of a 2/2 SL, the polarization can in principle be switched via a ($a^-a^-c^+$+ FEL) mode. The switching barrier can roughly be extracted from Figure 1(c). In a simple picture, switching of the $a^-a^-c^0$ mode in Pm ($a^-a^-c^+$) requires the structure to go through the intermediate *Cmmm* ($a^0a^0c^+$) phase [+ ($a^-a^-c^+$) → ($a^0a^0c^+$) → -($a^-a^-c^+$)]. Thus, the energy to switch is ΔE = E($a^0a^0c^+$)−E($a^-a^-c^+$). From Figure 1(c), ΔE=[E($a^0a^0c^+$)-E($a^-a^-c^0$)]-[E($a^-a^-c^+$)-E($a^-a^-c^0$)]∼(0.65 + 0.15)eV = 0.8 eV, is very high. Thus switching of $a^-a^-c^+$+ FEL is not likely.

In conclusion, in this paper we have investigated engineering a system where two distinct functional properties, metal-insulator transition and ferroelectricity, can coexist. We have chosen $La_{0.75}Sr_{0.25}MnO_3/LaNiO_3$ superlattices as a promising system since both of its building blocks are metallic in bulk form. We have found that an intermixed 2/2 SL can be ferroelclectic with a large spontaneous polarization. Small disproportionation of the oxidation state on Ni sites is found to be the origin of a metal-insulator transition, driving the system from ferroelectric-like metallic phase to ferroelectric insulating phase. The ferroelectric distortion persists even when the system is metallic and strongly depends on the carrier concentration, which can lead to the possibility of designing carrier-concentration tunable ferroelectrics. Finally, it will be interesting to investigate the strain dependence of the calculated properties, which can be addressed in future.

This work was supported by Department of Energy Grant number DE- FG02-09ER46554 (SG, STP) and by the Department of Energy Basic Energy Sciences, Materials Science and Engineering Directorate (AYB). The authors acknowledge NERSC supercomputing facility for providing computer time.

* saurabh.ghosh@vanderbilt.edu

[1] W. Knzig, Solid State Physics **4**, 5 (1957).
[2] W. Cochran, Phys. Rev. Lett. **3**, 412 (1959).
[3] P. W. Anderson and E. I. Blount, Phys. Rev. Lett. **14**, 217 (1965).
[4] Y. Shi, Y. Guo, X. Wang, A. J. Princep, D. Khalyavin, P. Manuel, Y. Michiue, A. Sato, K. Tsuda, S. Yu, M. Arai, Y. Shirako, M. Akaogi, N. Wang, K. Yamaura, and A. T. Boothroyd, Nat Mater **12**, 1024 (2013).
[5] N. A. Benedek and T. Birol, J. Mater. Chem. C **4**, 4000 (2016).
[6] M. S. J. Marshall, A. Malashevich, A. S. Disa, M.-G. Han, H. Chen, Y. Zhu, S. Ismail-Beigi, F. J. Walker, and C. H. Ahn, Phys. Rev. Applied **2**, 051001 (2014).
[7] H. M. Liu, Y. P. Du, Y. L. Xie, J.-M. Liu, C.-G. Duan, and X. Wan, Phys. Rev. B **91**, 064104 (2015).
[8] H. Sim and B. G. Kim, Phys. Rev. B **89**, 201107 (2014).
[9] G. Giovannetti and M. Capone, Phys. Rev. B **90**, 195113 (2014).
[10] D. Puggioni, G. Giovannetti, M. Capone, and J. M. Rondinelli, Phys. Rev. Lett. **115**, 087202 (2015).
[11] Y. Weng, J.-J. Zhang, B. Gao, and S. Dong, Phys. Rev. B **95**, 155117 (2017).
[12] M. Imada, A. Fujimori, and Y. Tokura, Rev. Mod. Phys. **70**, 1039 (1998).
[13] N. A. Benedek and C. J. Fennie, Phys. Rev. Lett. **106**, 107204 (2011).
[14] S. Ghosh, H. Das, and C. J. Fennie, Phys. Rev. B **92**, 184112 (2015).
[15] H. Zhang, Y. Weng, X. Yao, and S. Dong, Phys. Rev. B **91**, 195145 (2015).
[16] X. He and K.-j. Jin, Phys. Rev. B **93**, 161108 (2016).
[17] A. Ohtomo, D. A. Muller, J. L. Grazul, and H. Y. Hwang, Nature **419**, 378 (2002).
[18] A. Bhattacharya and S. J. May, Annual Review of Materials Research **44**, 65 (2014), http://dx.doi.org/10.1146/annurev-matsci-070813-113447.
[19] M. Gibert, P. Zubko, R. Scherwitzl, J. Íñiguez, and J.-M. Triscone, Nat Mater **11**, 195 (2012).
[20] Q. He, R. Ishikawa, A. R. Lupini, L. Qiao, E. J. Moon, O. Ovchinnikov, S. J. May, M. D. Biegalski, and A. Y. Borisevich, ACS Nano **9**, 8412 (2015), pMID: 26174591, http://dx.doi.org/10.1021/acsnano.5b03232.
[21] A. Bhattacharya, S. J. May, S. G. E. te Velthuis, M. Warusawithana, X. Zhai, B. Jiang, J.-M. Zuo, M. R. Fitzsimmons, S. D. Bader, and J. N. Eckstein, Phys. Rev. Lett. **100**, 257203 (2008).
[22] R. Mishra, Y.-M. Kim, J. Salafranca, S. K. Kim, S. H. Chang, A. Bhattacharya, D. D. Fong, S. J. Pennycook, S. T. Pantelides, and A. Y. Borisevich, Nano Letters **14**, 2694 (2014), pMID: 24734897, http://dx.doi.org/10.1021/nl500601d.
[23] W. Kohn and L. J. Sham, Phys. Rev. **140**, A1133 (1965).
[24] G. Kresse and D. Joubert, Phys. Rev. B **59**, 1758 (1999).
[25] V. I. Anisimov, I. Aryasetiawan, and A. I. Lichtenstein, Phys. Condens. Matter **9**, 767 (1997).
[26] A. I. Liechtenstein, V. I. Anisimov, and J. Zaanen, Phys. Rev. B **52**, R5467 (1995).
[27] G. Kresse and J. Furthmüller, Phys. Rev. B **54**, 11169 (1996).
[28] J. P. Perdew, A. Ruzsinszky, G. I. Csonka, O. A. Vydrov, G. E. Scuseria, L. A. Constantin, X. Zhou, and K. Burke, Phys. Rev. Lett. **100**, 136406 (2008).
[29] T. Akimoto, Y. Maruyama, Y. Moritomo, A. Nakamura, K. Hirota, K. Ohoyama, and M. Ohashi, Phys. Rev. B **57**, R5594 (1998).
[30] A. Urushibara, Y. Moritomo, T. Arima, A. Asamitsu, G. Kido, and Y. Tokura, Phys. Rev. B **51**, 14103 (1995).
[31] S. Johnston, A. Mukherjee, I. Elfimov, M. Berciu, and G. A. Sawatzky, Phys. Rev. Lett. **112**, 106404 (2014).
[32] M. L. Medarde, Journal of Physics: Condensed Matter **9**, 1679 (1997).
[33] B. Lau and A. J. Millis, Phys. Rev. Lett. **110**, 126404 (2013).
[34] P. Lee, V. Singh, G. Guo, H.-J. Liu, J.-C. Lin, Y.-H. Chu, C. Chen, and M.-W. Chu, Nature Communications **7**, 12773 (2016).
[35] A. T. Lee and M. J. Han, Phys. Rev. B **88**, 035126 (2013).
[36] J. Hoffman, I. C. Tung, B. B. Nelson-Cheeseman, M. Liu, J. W. Freeland, and A. Bhattacharya, Phys. Rev. B **88**, 144411 (2013).
[37] M. Gibert, M. Viret, A. Torres-Pardo, C. Piamonteze, P. Zubko, N. Jaouen, J.-M. Tonnerre, A. Mougin, J. Fowlie, S. Catalano, A. Gloter, O. Stphan, and J.-M. Triscone, Nano Letters **15**, 7355 (2015), pMID: 26484628, http://dx.doi.org/10.1021/acs.nanolett.5b02720.
[38] J. D. Hoffman, B. J. Kirby, J. Kwon, G. Fabbris, D. Meyers, J. W. Freeland, I. Martin, O. G. Heinonen, P. Steadman, H. Zhou, C. M. Schlepütz, M. P. M. Dean, S. G. E. te Velthuis, J.-M. Zuo, and A. Bhattacharya, Phys. Rev. X **6**, 041038 (2016).
[39] A. M. Glazer, Acta Crystalogr A **31**, 756 (1975).
[40] A. T. Lee and M. J. Han, Phys. Rev. B **88**, 035126 (2013).
[41] H. Das, U. V. Waghmare, T. Saha-Dasgupta, and D. D. Sarma, Phys. Rev. Lett. **100**, 186402 (2008).